JOURNAL OF APPLIED ELECTROCHEMISTRY **28** (1998) 855–862

Optimization of bath composition for hard Fe–C alloy plating

Y. FUJIWARA, M. IZAKI, H. ENOMOTO

Osaka Municipal Technical Research Institute, 1-6-50, Morinomiya, Joto-ku, Osaka, 536 Japan

T. NAGAYAMA*, E. YAMAUCHI

Department of Materials Science and Engineering, Kansai University, 3-3-5, Yamate-cho, Suita-city, Osaka, 564 Japan

A. NAKAE

Fuso Chemical Co. Ltd, 2-2-6, Niitaka, Yodogawa-ku, Osaka, 532 Japan

Received 20 April 1997; revised 18 August 1997

Fairly uniform Fe–C alloy deposits with bright appearance and characteristic black colour were obtained in Hull cell tests at 1.0 A from baths with the following composition: $FeSO_4$ 0.5 M or higher, citric acid 0.01 M or lower, and pH around 2.0. The carbon content of the deposits from these baths ranged between 1.0 and 1.2 wt % and the Vickers hardness was HV 700 or above over a wide area of the Hull cell cathode. The thickness distribution of the deposits on the Hull cell cathode from these baths suggested that the current efficiency was 100% and the local current density obeyed the primary current distribution, except for the region near the low-current-density (LCD) end where the thickness decreased unexpectedly. The addition of chloride ion as NaCl, at concentrations of 1.0 M or above, improved the thickness in the LCD region, and the thickness distribution on the Hull cell cathode suggested that current efficiency was 100% even at the LCD end. Chloride ion did not affect the carbon content or the hardness of the deposits. Polarization measurements showed that the hydrogen ion reduction occurred at more noble potentials than Fe deposition. The unexpected thickness decrease near the LCD end, observed in Hull cell tests, and the improvement of this by adding chloride ion were both accounted for by the change in the preceding hydrogen ion reduction rate. The increase in citric acid concentration enhanced hydrogen ion reduction and therefore caused a lowering of current efficiency at low current densities. On the other hand, the addition of chloride ion inhibited hydrogen ion reduction and caused an increase in current efficiency at low current density.

Keywords: *electroplating*, *Fe–C alloys*, *hard deposits*, *bath composition*, *covering power*, *effects of chloride*

---

1. Introduction

Fe electroplating has been used for various engineering applications such as glass moulds, soldering iron tips, electroforming and repairing worn parts, where wear resistance is required [1, 2]. Nevertheless, fairly low Vickers hardness of the electroplated Fe ranging from HV 150 to HV 500 [1] leads to insufficient wear resistance.

Izaki *et al.* [3] reported that hard Fe-carbon alloys can be electrodeposited from dilute aqueous solution of $FeSO_4$ with citric acid and L-ascorbic acid. The composition of Izaki's solution [3] was as follows: 0.14 M $FeSO_4$, 5.7 mM citric acid and 17 mM L-ascorbic acid. The electrodeposited Fe–C alloys contain 1.0 wt% carbon, show a Vickers hardness around HV 800, a smooth surface and a black colour, and have a body-centred tetragonal martensite type lattice [3–5]. Similar Fe–C alloys were also electrodeposited from dilute $FeSO_4$ solutions containing L-malic acid, succinic acid, citric acid or adipic acid without the addition of L-ascorbic acid [6, 7]. Fe–C alloy electrodeposition is an attractive alternative process to Fe electroplating because of the high hardness of the deposits. It also has potential as an alternative to Cr plating, electroless Ni–P plating and thermal surface hardening processes such as carburizing because the hardness of the deposits is comparable to those produced by these processes.

However, Izaki's solution would have serious disadvantages for commercial applications because of its low Fe^{2+} concentration and low ionic strength. The

---

* Present address: Kyoto Municipal Institute of Industrial Research, 17 Chudoji Minami-machi, Shimogyo, Kyoto, 600 Japan.

0021-891X

low Fe^{2+} concentration would give burnt deposits at high current densities and therefore cause a narrow operating range. A change in the solution composition during continuous operation is also expected. The low ionic strength causes low electrical conductivity of the solution and, therefore, leads to an extremely high bath voltage. This also causes poor throwing power [8] and resultant nonuniform deposit thickness distribution due to nonuniform current distribution on substrates of irregular profile. Current distribution will be more uniform in solutions with higher electrical conductivity and/or higher polarization resistance of the electrodeposition reaction [9, 10].

The aim of this work is to propose an optimum bath composition for hard Fe–C alloy plating for commercial use. Citric acid was chosen as the carbon source. The most important factors for the commercial use are whether the deposits on an irregular substrate have uniform surface morphology and thickness as well as uniformly high hardness. A standard 267 cm^3 Hull cell [11] was used to study the uniformity of the Fe–C alloy deposits on an irregular substrate. In particular, the effects of Fe^{2+} and citric acid concentration on the uniformity of the deposits were studied. The effects of the addition of Na_2SO_4 and NaCl as supporting electrolytes were also studied. The role of chloride ions in the electrodeposition processes is discussed on the basis of polarization behaviour.

2. Experimental details

Baths were prepared from reagent grade chemicals and deionized distilled water, and contained various concentrations of $FeSO_4$ and citric acid. The effects of the addition of Na_2SO_4 and NaCl as supporting electrolytes were also studied. The bath pH was not adjusted unless otherwise noted, and ranged from 1.7 to 2.2. In the experiments where the effects of the bath pH were studied, H_2SO_4 was used to lower the pH, and a mixture of citric acid and trisodium citrate with additional NaOH, if necessary, was used to raise the pH. Bath temperature was 50 ± 1 °C, unless otherwise noted, and the bath was not agitated. Dissolved oxygen concentration was determined at room temperature using a DO-meter (OM-14, Horiba Ltd).

Dissolved oxygen concentration of the $FeSO_4$-citric acid solutions was less than 0.5 ppm, although that of the water used as solvent was around 8 ppm. Dissolved oxygen was consumed for oxidizing Fe^{2+}; this reaction would be fast because Fe^{3+}-citrate complexes [12] are stable. The currents due to the reduction of dissolved oxygen, therefore, need not be considered even in cyclic voltammetry measurements. Experiments were thus done under an air atmosphere throughout this work.

Electrical conductivities of the solutions were measured at 50 °C using a conductivity meter (CM-15A, Toa Electronics Ltd).

A standard 267 cm^3 Hull cell [11] was used to estimate the uniformity of the deposits on substrates having macroscopic irregularities. The cathode was an oxygen-free, high-conductivity Cu sheet 100 μm thick. The cathodes were degreased by cathodic electrolysis in an aqueous solution containing 100 $g\,dm^{-3}$ $K_4P_2O_7$ and 50 $g\,dm^{-3}$ KOH, dipped in a diluted H_2SO_4 solution and rinsed with deionized distilled water just before electrodeposition. The anode was a mild steel sheet in an anode bag. The total applied current was 1.0 A. The charge was 600 C for the evaluation of the uniformity of appearance, and 5000 C for the evaluation of thickness, hardness and carbon content distribution.

To make the samples for the determination of thickness and hardness distribution, nickel was plated from a Watts bath onto the deposits as a protection layer for cutting and polishing. Ni-plated samples were first cut away in 5 mm areas both from the high- and the low-current density ends and cut into nine strips 10 mm in width. Each strip was mounted in acrylic resin and polished with alumina powder for microscopic examination and for hardness measurements of the cross section of the deposits. Thickness of the deposits was measured by the examination of the cross section with an optical microscope (Optiphot, Nikon).

Hardness measurements of the deposits were made using a micro Vickers hardness tester (Type M, Shimadzu) with a load of 25 g. Hardness was measured at 10 positions or more for each strip. The average value and the 95% confidence limit of the hardness were determined.

The carbon content of the deposits was determined using a carbon analyser (EMIA-1110, Horiba, Ltd), measuring the amount of CO_2 evolved by high-frequency induction heating of samples in an oxygen atmosphere. The samples for carbon analysis were 10 mm wide strips cut from the Fe–C alloy-deposited Hull cell cathode in the same manner as that for the cross-section examination. Therefore, the carbon content of the deposit at each point of a Hull cell cathode shows the average value in a region 5 mm apart on both sides. The oxygen-free, high-conductivity copper substrate essentially did not contain any carbon.

Electrodeposition at constant current densities was also carried out for 100 C in a one-component Pyrex glass cell having a volume of 300 cm^3. The effects of current density on current efficiency, carbon content, surface morphology and crystal structure of the deposits were studied. The cathode was an oxygen-free, high-conductivity copper sheet or a stainless steel sheet mounted in an acrylic resin electrode holder and having an exposed area of 1 cm^2. The anode was a large area mild steel sheet.

Current efficiency was determined from the weight of the deposits obtained at a given amount of charge assuming that only Fe was deposited from Fe^{2+}; this assumption is valid because of the relatively low carbon content of the deposits. Surface morphology of the deposits was examined using a scanning electron microscope (SEM, JSM T-100, Jeol Co.). Deposits obtained on a stainless steel sheet were mechanically removed from the substrate and powdered for X-ray diffraction measurements. X-ray diffraction measurements were made using an X-ray diffractometer system (MXP-18, MAC Science) and monochromated CuK_α at 50 kV, 200 mA.

Polarization behaviour was measured on a mild steel electrode under quasisteady state condition, that is, by the potential sweep method with a very slow sweep rate of 0.5 mV s^{-1}. The reference electrode was a Ag/AgCl electrode in a saturated KCl solution (Ag/AgCl (sat. KCl)) connected to the cell by a Luggin capillary near the working electrode. The counter electrode was a large area mild steel sheet. The electrodes were connected to a potentiostat/galvanostat (HA-501G, Hokuto Denko) in conjunction with a function generator (HB-105, Hokuto Denko) and a personal computer. The potential sweep was made cathodically from the immersion potential.

Cyclic voltammetry at a high sweep rate of 50 mV s^{-1} was made for a Pt electrode at 25 °C. The reference electrode was the same as that used in the polarization measurements at a slow sweep rate but the counter electrode was a large area platinized titanium sheet. Steady-state cyclic voltammograms were recorded between −1.2 and + 1.3 V vs Ag/AgCl (sat. KCl) after at least 20 cycles.

The pretreatment procedures of the working electrodes for polarization and cyclic voltammetry measurements were the same as those of the Hull cell cathode.

3. Results and discussion

3.1. *Uniformity of the deposits: Hull cell experiments*

3.1.1. Appearance. Figure 1 shows schematic representations of the appearance of the electrodeposits obtained in Hull cell experiments. The effects of Fe^{2+} concentration are shown in Fig. 1(A), (B) and (C). Citric acid concentration was 0.01 M. A burnt area due to the 'black oxide' [6] precipitation was observed at the high current density (HCD) region when the Fe^{2+} concentration was 0.2 M or lower. The burnt area was decreased with increasing Fe^{2+} concentration and disappeared when it was 0.5 M or above. From these high-Fe^{2+} baths, bright deposits of black colour were obtained almost over the whole area of a Hull cell cathode except for the narrow region near the low-current-density (LCD) end, where the appearance was dull and greyish independent of Fe^{2+} concentration.

Bath voltages during Hull cell tests were higher than 10 V when the Fe^{2+} concentration was below 0.2 M; this is an extremely high value that leads to a serious disadvantage when the process is operated on a large scale. The bath voltages declined dramatically with increasing Fe^{2+} concentration and were around 4 V when the Fe^{2+} concentration was 0.5 M or above.

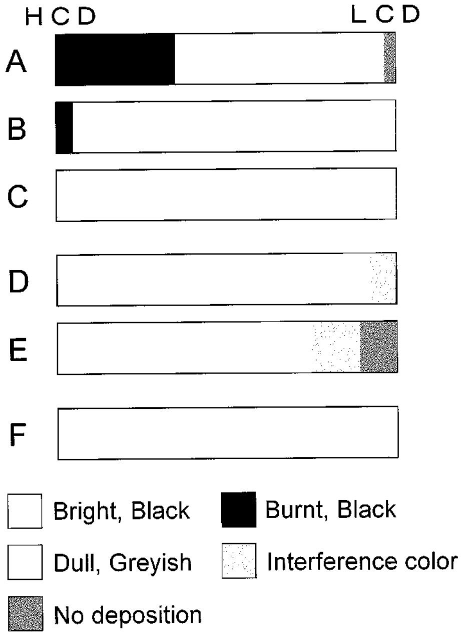

Fig. 1. Schematic representations of the appearance of the deposits in Hull cell experiments. Bath compositions: (A) $FeSO_4$ 0.1 M, citric acid 0.01 M; (B) $FeSO_4$ 0.2 M, citric acid 0.01 M; (C) $FeSO_4$ 0.5 M, citric acid 0.01 M; (D) $FeSO_4$ 0.5 M, citric acid 0.025 M; (E) $FeSO_4$ 0.5 M, citric acid 0.1 M; (F) $FeSO_4$ 0.5 M, citric acid 0.01 M, NaCl 1.5 M. Key: (HCD) high-current density end; (LCD) low-current density end.

The effects of citric acid concentration on the appearance of the deposits can be seen from a comparison of Fig. 1(C), (D) and (E). The Fe^{2+} concentration was 0.5 M. The appearance of the Fe deposit from the bath without citric acid is not shown in Fig. 1 but was dull and greyish over the whole area of the cathode. The addition of 0.01 M of citric acid to the bath produced a bright, black appearance of the deposits characteristic of the Fe–C alloy deposits [3] over a large area on the cathode as shown in Fig. 1(C). However, with increasing citric acid concentration, a narrow region with a dull, greyish appearance near the LCD end spread toward the HCD part. A region with interference colour and that without deposits also appeared at the LCD region (Fig. 1(D) and (E)), showing that the metallic Fe or Fe–C alloys were very thin or were essentially not deposited. Bath voltages were not practically affected by citric acid concentration and were 4 V or below when the Fe^{2+} concentration was 0.5 M or above.

Consequently, the Fe^{2+} concentration should be 0.5 M or above and the citric acid concentration should be 0.01 M or below to obtain fairly uniform Fe–C alloy deposits onto a Hull cell cathode with relatively low bath voltages. However, the nonuniformity of the deposits near the LCD end was unavoidable.

Addition of NaCl to the high-Fe^{2+} low-citric acid baths (HFLC bath) further improved the uniformity of the deposits and decreased bath voltage. Figure 1(F) shows a typical result from the bath with NaCl. By adding more than 1.0 M NaCl, the narrow area with grey or interference colour near the LCD region disappeared, and the deposits exhibited a bright appearance and black colour over the entire Hull cell cathode. On the other hand, the addition of Na_2SO_4 to the HFLC baths did not affect the appearance of the deposits. Bath voltages were further decreased and were 2.0 V or below when the NaCl concentration was 1.0 M or above. The decrease in bath voltage with increasing NaCl concentrations is attributed to the increase in electrical conductivity of the solutions. For example, the electrical conductivity of the solution containing 0.5 M $FeSO_4$ and 0.01 M citric acid without NaCl was 45.8 mS cm^{-1}, while that of the solution with 2.0 M NaCl was 212 mS cm^{-1}.

3.1.2. Effects of supporting electrolytes on thickness distribution: throwing power and covering power. Figure 2 shows thickness distributions of the deposits on a Hull cell cathode from the baths containing 0.5 M $FeSO_4$ and 0.01 M citric acid with and without 1.5 M NaCl. The dashed line indicates the calculated thickness distribution assuming that the local current density obeys the primary current distribution, the current efficiency is 100%, and the density of the deposit is equal to that of the bulk pure Fe. An analytic solution by West *et al.* [13] was used to calculate the primary current distribution on the Hull cell cathode. The thickness distributions of these two deposits both suggest that current efficiency is practically 100% over a wide area of the cathode and that local current density is represented by the primary current distribution. The addition of NaCl did not make the current distribution more uniform; that is, it did not increase the throwing power, although it raised the electrical conductivity of the solution.

A sharp decrease in thickness in the 2 cm region from the LCD end was observed in the deposits from the bath without NaCl. However, the addition of NaCl improved the deposit thickness in the LCD region, suggesting that current efficiency practically attained 100% even at the LCD end. The increase in current efficiency in the LCD region corresponds with the improvement of the uniformity of appearance of the deposits on adding NaCl. The ability to produce any deposits at all at the LCD region of an irregular substrate such as in a recess is generally called covering power [8]. The addition of NaCl improved the covering power.

The covering power was not improved at all by adding Na_2SO_4, although bath voltages declined as with the addition of NaCl. Therefore, chloride ion is responsible for the improved uniformity of the deposits from the bath with NaCl.

3.1.3. Distribution of carbon content and hardness of the deposits. Figure 3 shows the distribution of the carbon content of the deposits on a Hull cell cathode. The carbon content of the deposits ranged between 1.0 and 1.2 wt % over a wide area of the HCD and moderate current density (MCD) regions, and decreased near the LCD end. The addition of NaCl to the bath had little effect on the carbon content distribution of the deposits.

Figure 4 shows the hardness distribution of the Fe–C alloy deposits on a Hull cell cathode from the baths with and without NaCl. The hardness distribution of the Fe deposit from a 1.0 M $FeSO_4$ solution is also shown. The hardness of the Fe deposit was below HV 400 over the entire cathode, showing typical values of Fe electrodeposits [1]. In contrast, the Fe–C alloy deposits obtained from the baths with and without NaCl both exhibited a high hardness of HV 700 or above over almost the entire cathode. These values are characteristic of the Fe–C alloy electrodeposits containing 0.6 to 1.2 wt % carbon [5, 7] and therefore correspond with the carbon content distribution of the deposits on a Hull cell cathode, which is 0.6 wt % or above as shown in Fig. 3. The

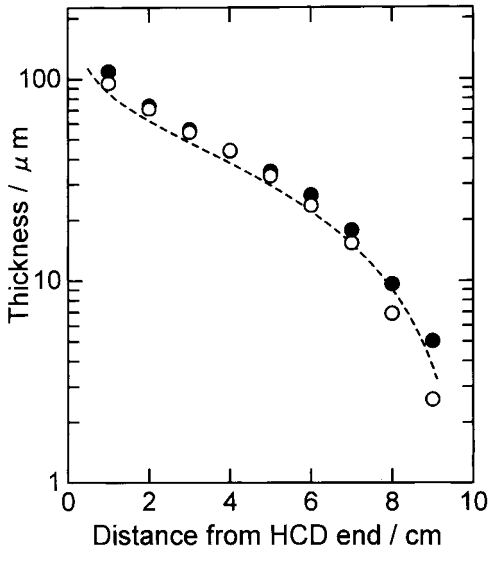

Fig. 2. Thickness distribution of the deposits on a Hull cell cathode. (----) calculated values assuming the primary current distribution [13] and the 100% current efficiency; Bath compositions: (○) $FeSO_4$ 0.5 M, citric acid 0.01 M; (●) $FeSO_4$ 0.5 M, citric acid 0.01 M, NaCl 1.5 M.

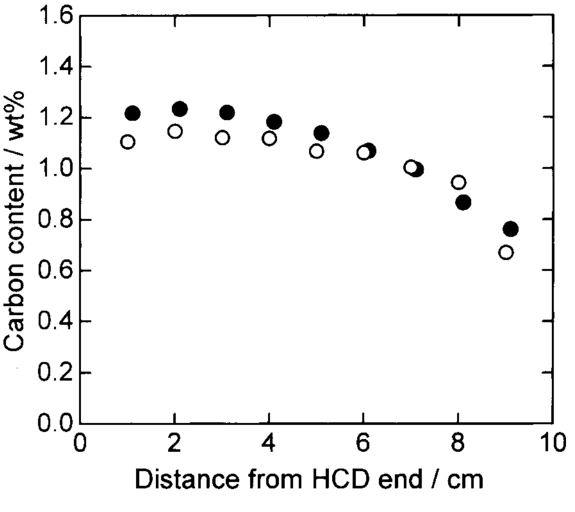

Fig. 3. Distribution of the carbon content of the deposits on a Hull cell cathode. Bath compositions: (○) $FeSO_4$ 0.5 M, citric acid 0.01 M; (●) $FeSO_4$ 0.5 M, citric acid 0.01 M, NaCl 1.5 M.

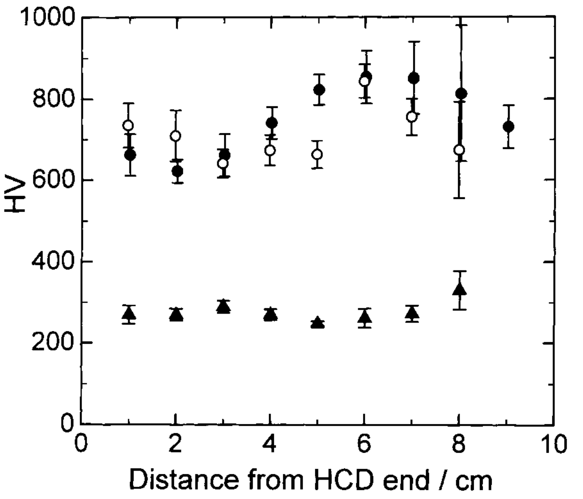

Fig. 4. Hardness distribution of the deposits on a Hull cell cathode. Bath compositions: (○) $FeSO_4$ 0.5 M, citric acid 0.01 M; (●) $FeSO_4$ 0.5 M, citric acid 0.01 M, NaCl 1.5 M; (▲) $FeSO_4$ 1.0 M. Error bars represent the 95% confidence limit.

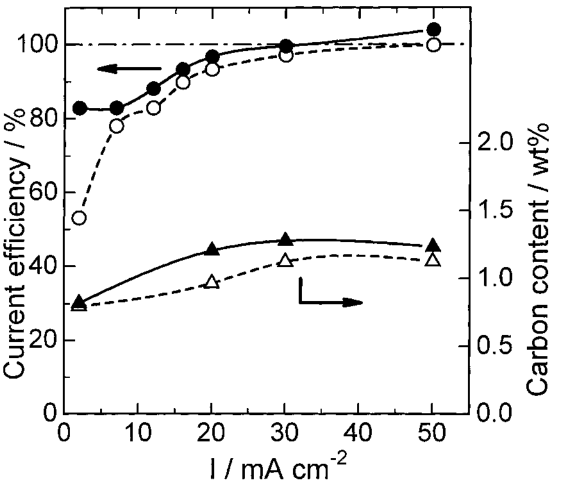

Fig. 5. Effects of current density on current efficiency and the carbon content of deposits. Bath compositions: (○, △) $FeSO_4$ 0.5 M, citric acid 0.01 M; (●, ▲) $FeSO_4$ 0.5 M, citric acid 0.01 M, NaCl 1.5 M. Key: (○, ●) current efficiency; (△, ▲) carbon content.

addition of NaCl to the bath did not lower the carbon content or hardness of the deposits on the whole area of the Hull cell cathode.

3.2. *Current efficiency, carbon content, morphology and crystal structure of the deposits: constant current density experiments*

Figure 5 shows the effects of current density on current efficiency and the carbon content of the deposits from the HFLC baths with and without NaCl. From both these baths, Fe–C alloys containing about 1 wt % carbon were deposited at high current efficiencies near 100% over a wide range of current density. Current efficiency was decreased at low current densities and this was improved by the addition of NaCl; current efficiency of the bath with NaCl was higher than 80% even at 2.0 mA cm^{-2}. These results coincide with the results of Hull cell experiments; the addition of NaCl improved the unexpectedly small thickness near the LCD end, and thus thickness distribution was almost the same as that assumed with 100% current efficiency over a wide area of the Hull cell cathode.

Figure 6 shows SEM photographs of the surface of the Fe–C alloy deposits obtained from the HFLC baths with and without NaCl. Surface morphology of the deposits at an extremely low current density of 2.0 mA cm^{-2} was angular-grained, characteristic of Fe deposits [4] and the Fe–C alloy deposits of which the carbon content is lower than 0.5 wt % [4, 6, 7]. This coincides with the decrease in carbon content at low current densities. The size of the grains was slightly larger in the deposits from the bath with NaCl than that without NaCl. On the other hand, at moderate current densities up to 50 mA cm^{-2},

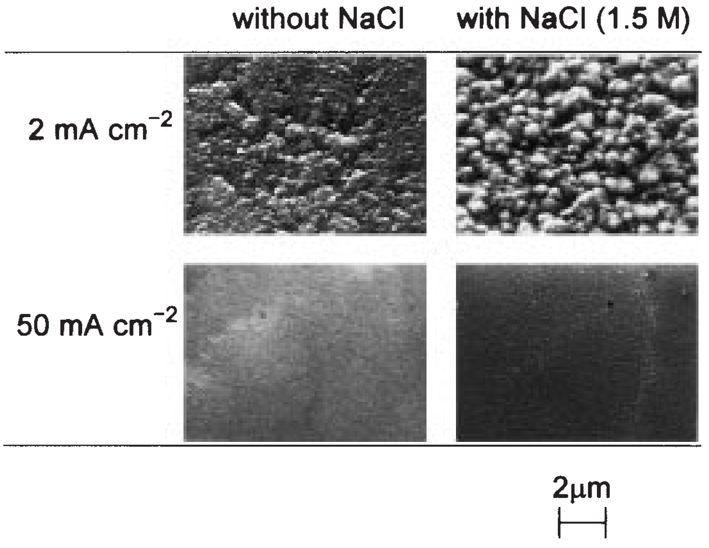

Fig. 6. SEM photographs of the surface of the Fe–C alloy deposits. Bath compositions: (left hand) $FeSO_4$ 0.5 M, citric acid 0.01 M; (right hand) $FeSO_4$ 0.5 M, citric acid 0.01 M, NaCl 1.5 M.

extremely smooth deposits were obtained from both the baths with and without NaCl.

Figure 7 shows the powder X-ray diffraction patterns of the Fe–C alloy deposits at 50 mA cm^{-2}. The patterns were practically unchanged on adding NaCl to the bath, and all the diffraction peaks were apparently assigned to α-Fe [14]. The width of every diffraction peak was large and the features were asymmetric, as clearly seen in the extended profiles around the (2 1 1) peak. This is attributed to the peak splitting into the (1 1 2) peak appearing at lower 2θ and the (2 1 1) peak at higher 2θ due to the tetragonal martensite type structure according to the detailed discussion in the previous papers [4–7]. It is well-known that Fe–C martensite has a body-centred tetragonal lattice and is an interstitial solid solution with carbon on the octahedral site. Its lattice constants were close to those of α-Fe (a body centred cubic lattice) but its axial ratio slightly increased with increasing carbon content [15].

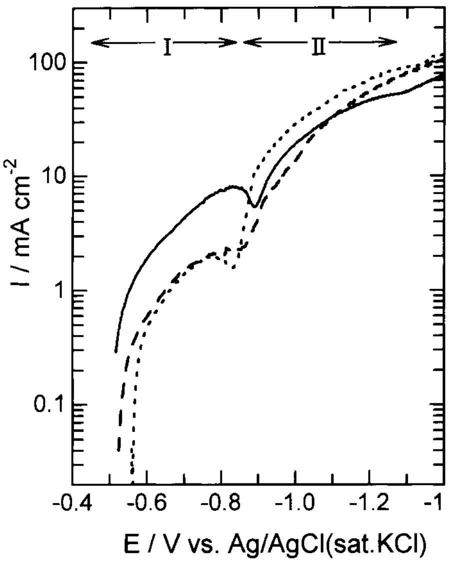

Fig. 8. Cathodic polarization curves under quasi-steady state condition (potential sweep rate 0.5 mV s^{-1}). (······) $FeSO_4$ 1.0 M, pH 2.0; (----) $FeSO_4$ 1.0 M, citric acid 0.025 M, pH 2.0; (—) $FeSO_4$ 1.0 M, citric acid 0.1 M, pH 2.0.

3.3. *Polarization behaviour*

Figure 8 shows the cathodic polarization curves of the 1.0 M $FeSO_4$ solutions with and without citric acid by the potential sweep method with a slow sweep rate of 0.5 mV s^{-1}. The solutions were adjusted to pH 2.0 to equalize the hydrogen ion activity. These polarization curves can be divided into two regions. First, the current rises sharply at around −0.5 V vs Ag/AgCl (sat. KCl) and reaches a plateau at around −0.8 V (region I). Second, the cathodic current rises again at around −0.9 V (region II).

In the potential region I, where the limiting currents increased with increasing citric acid concentration, current is mainly attributed to hydrogen ion reduction. This is because the limiting current at pH 2.0 was one tenth of that of the solution with the same citric acid concentration at pH 1.0, in agreement with the factor of ten difference in hydrogen ion activity, as shown in Fig. 9. However, at higher pHs, a decrease in the limiting currents with the rise of the solution pH was more slower than expected from the linear dependence between hydrogen ion activity and the limiting current. The limiting currents approached 0.1 or 0.2 mA cm^{-2} at higher pH. This suggests that the limiting currents at higher pH show the diffusion-limited current of the reduction of a trace amount of Fe^{3+} to Fe^{2+}, as pointed out by Horkans [16].

The limiting currents in the solutions with citric acid are obviously higher than those without citric acid at around pH 3.0 as shown in Fig. 9. This pH is near the p*K* value of the first dissociation of citric acid, $pK_a = 3.13$ [12], corresponding to the pH value where the greatest buffer capacity is expected [17]. In other words, at around pH 3, citric acid can dissociate

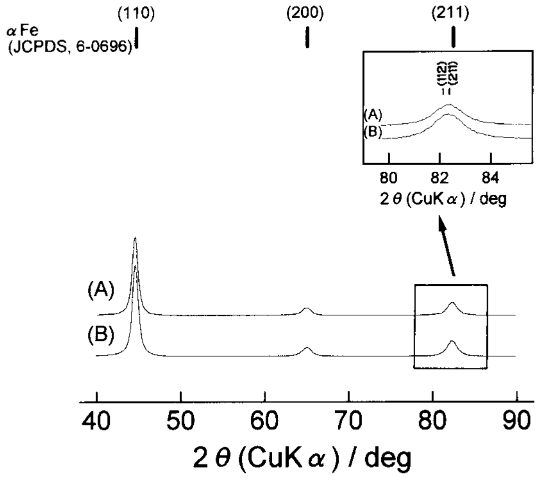

Fig. 7. Powder X-ray diffraction patterns of the Fe–C alloy deposits. Bath compositions: (A) $FeSO_4$ 0.5 M, citric acid 0.01 M; (B) $FeSO_4$ 0.5 M, citric acid 0.01 M, NaCl 1.5 M; current density: 50 mA cm^{-2}.

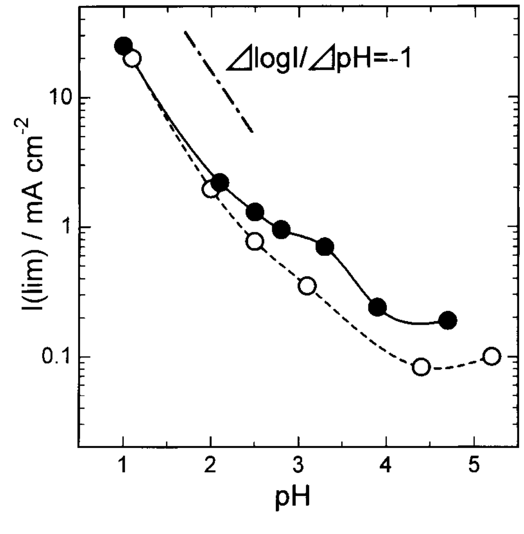

Fig. 9. Relationship between the solution pH and the limiting current density in the region I of the cathodic polarization curves at 0.5 mV s^{-1}: (○) $FeSO_4$ 1.0 M; (●) $FeSO_4$ 1.0 M, citric acid 0.025 M.

a large number of protons with the pH rise at the cathode surface and therefore can contribute to the increase in the current of hydrogen ion reduction. Horkans [16] also reported that citric acid solution exhibited an exceptionally large limiting current of hydrogen ion reduction reaction at around pH 3 and claimed that this is attributed to a sufficiently high dissociation rate of citric acid. The increase in citric acid concentration enhances the hydrogen ion reduction rate as shown in Fig. 8, and this leads to the worsening of the covering power as shown in Fig. 1(E).

In the potential region II shown in Fig. 8, the rise in current shows the onset of Fe electrodeposition. The Fe deposition reaction was inhibited by citric acid. This is correlated to the Fe–C alloy deposition mechanisms from the baths with organic acids. During electrodeposition of Fe–C alloys, black oxide films of several tens of nanometres thick comprising FeO and carboxyls were present at the cathode surface, and Fe–C alloys were deposited through the black oxide films [6, 7]. The black oxide films inhibited Fe deposition.

The effects of chloride ion on polarization behaviour were not significant under quasisteady state conditions but were obviously observed in cyclic voltammograms at a faster sweep rate. Figure 10 shows the cyclic voltammograms at 50 mV s^{-1} for a Pt electrode in Fe^{2+}-citric acid solutions with and without 1.0 M NaCl. The solution pHs were adjusted to 2.0. The rise in cathodic currents at around −1.0 V vs Ag/AgCl (sat. KCl) (C2) indicates Fe–C alloy electrodeposition, and the deposited alloys are stripped off by anodic dissolution on the anodic sweep between −0.6 and −0.2 V (A1). The area under the stripping peak corresponds to the charge required to oxidize the deposited Fe and is proportional to the average deposition rate for a cycle. The addition of NaCl made the rise in cathodic current sharper and, corresponding to this, the stripping peak area became significantly larger. This shows that chloride ion enhances Fe–C alloy deposition. The enhancement of Fe–C alloy deposition can be explained by the catalysis of electron transfer by the Cl$^-$ bridge between Fe^{2+} and the cathode surface as in the discussion on Fe and Ni electrodeposition by Horkans [16]. Stoichev *et al.* [18] also proposed that Cu electrodeposition is catalysed by a Cl$^-$ bridge.

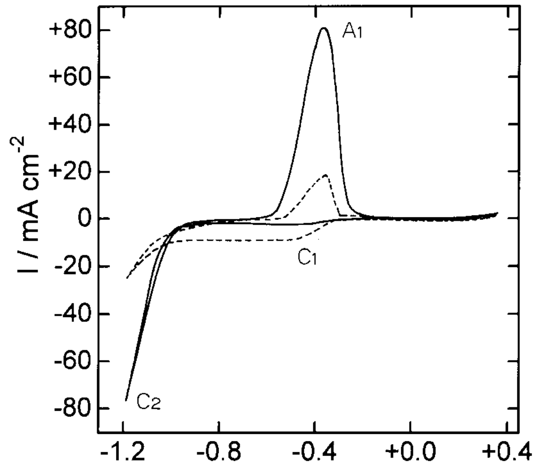

Fig. 10. Cyclic voltammograms at 50 mV s^{-1} for a Pt electrode: (----) FeSO$_4$ 0.5 M, citric acid 0.01 M, pH 2.0; (—) FeSO$_4$ 0.5 M, citric acid 0.01 M, NaCl 1.5 M, pH 2.0.

The addition of chloride ion to the bath did not improve the throwing power, although the electrical conductivity of the solution was increased [9, 10], as described before. This is due to the decrease in polarization resistance, that is, the enhancement of Fe electrodeposition by adding chloride ion, as suggested from the sharper rise in Fe–C alloy deposition current in the solution with NaCl than that in the solution without NaCl shown in Fig. 10.

A cathodic current plateau due to hydrogen ion reduction on the Pt electrode was observed at −0.5 to −1.0 V vs Ag/AgCl (sat. KCl) (Cl in Fig. 9), more noble potentials than those where Fe–C alloy deposition occurred (C2). The addition of NaCl significantly reduced the limiting current of hydrogen ion reduction. The inhibition of hydrogen ion reduction current is responsible for the improvement in the covering power, shown in Fig. 2 as the larger thickness of the deposits in the LCD region of a Hull cell cathode. Horkans [16] reported similar results for the limiting current of hydrogen ion reduction and attributed this to the smaller diffusion coefficient of hydrogen ion in a solution with chloride ion than in a solution with sulfate ion. Another mechanism can also explain the decrease in hydrogen ion reduction current on adding chloride ion; that is, the specifically adsorbed chloride ion [19] decreases the active surface area for hydrogen atoms to adsorb after reduction. Adsorbed hydrogen atoms are the intermediate of hydrogen gas evolution.

4. Conclusions

An optimum bath composition for hard Fe–C alloy plating was determined in view of the uniformity of the deposits on substrates of irregular profile. The baths were the modified Izaki's solution, which was first proposed to obtain hard Fe–C alloy deposits and contained FeSO$_4$ as the iron source and citric acid as the carbon source. Uniformity of the deposits was evaluated from the Hull cell experiments at a total current of 1.0 A and at 50 °C. Fairly uniform Fe–C alloy deposits with a bright appearance and characteristic black colour were obtained with relatively low bath voltage around 4 V when the FeSO$_4$ concentration was 0.5 M or above and citric acid was 0.01 M or below. Therefore, the high-Fe^{2+}, low-citric acid (HFLC) bath is suitable to obtain uniform deposits on irregular substrates whereas a narrow dull region near the LCD end was unavoidable. The thickness distribution of the deposits on a Hull cell cathode from the HFLC bath suggested that the current effciency was almost 100% in the MCD and HCD regions and that the local current density obeyed the primary current distribution; whereas, a significant decrease in thickness of the deposits was observed near the LCD end.

However, the addition of NaCl of more than 1.0 M improved the uniformity of the deposits; that is, the deposits exhibited a bright appearance and black colour over the entire Hull cell cathode. The addition of NaCl further lowered the bath voltage. The addition of NaCl improved the thickness near the LCD end; that is, it improved the covering power. On the other hand, the addition of Na_2SO_4 did not show these effects, and therefore, it can be concluded that chloride ion is responsible for the improvement in the covering power.

The carbon content of the deposits from the HFLC bath ranged from 1.0 wt % to 1.2 wt % over a wide area of the Hull cell cathode and decreased near the LCD end. Hardness of the deposits was HV 700 or above over almost the entire Hull cell cathode, showing typical values of Fe–C alloy electrodeposits. Chloride ion in the bath had little effect on the carbon content or the hardness of the deposits.

SEM examination showed that the surface of the deposits from the HFLC bath was extremely smooth at current densities up to $50\,\mathrm{mA\,cm^{-2}}$, except for that obtained at $2.0\,\mathrm{mA\,cm^{-2}}$ or below. The structure of the deposits from the HFLC baths was a body-centred tetragonal martensite type, similar to those from the dilute Izaki's solution, on the basis of X-ray diffraction measurements. Consequently, an optimum composition of the HFLC bath to obtain uniform, hard Fe–C alloy deposits is as follows; Fe^{2+} is 0.5 M or above, citric acid 0.01 M or below, and chloride ion 1.0 M or above.

Polarization measurements showed that hydrogen ion reduction occurs at more noble potentials than Fe or Fe–C alloy deposition. The preceding hydrogen ion reduction is responsible for the worsening of the covering power. The limiting currents of hydrogen ion reduction were higher in the solution with the higher citric acid concentration, if the pH was the same. Therefore, the lower citric acid concentration is favorable for obtaining deposits with a higher covering power. The addition of chloride ion drastically decreased the limiting current of the preceding hydrogen ion reduction, and this led to the improvement in the covering power. Moreover, chloride ion enhanced Fe–C alloy deposition. These effects can be accounted for by the specifically adsorbed chloride ion, which decreases the active site for hydrogen atoms to adsorb and catalytically enhances the electron transfer to Fe^{2+} through the Cl^- bridge.

Acknowledgements

The authors wish to thank Satoshi Matsui for his experimental assistance.

References

[1] W. H. Safranek, 'The Properties of Electrodeposited Metals and Alloys', 2nd edn, American Electroplaters and Surface Finishers Society, Orlando (1986), p. 195.

[2] M. Borruso, *Plat. Surf. Finish.* **79**(5) (1992) 112.

[3] M. Izaki, H. Enomoto and T. Omi, *Hyomem Gijutsu (J. Surf. Fin. Soc. Japan)* **40** (1989) 1304.

[4] *Idem, Nihon Kinzoku Gakkaishi (J. Japan Inst. Metals)* **56** (1992) 636.

[5] M. Izaki and T. Omi, *Metall. Mater. Trans.* **27A** (1996) 483.

[6] Y. Fujiwara, M. Izaki, H. Enomoto and A. Nakae, *Denki Kagaku* **61** (1993) 840.

[7] Y. Fujiwara, T. Nagayama, A. Nakae, M. Izaki, H. Enomoto and E. Yamauchi, *J. Electrochem. Soc.* **143** (1996) 2584.

[8] F. A. Lowenheim, 'Electroplating', McGraw-Hill, New York (1978), p. 147.

[9] C. Wagner, *J. Electrochem. Soc.* **98** (1951) 116.

[10] M. Matlosz, C. Creton, C. Clerc and D. Landolt, *ibid*, **134** (1987) 3015.

[11] F. A. Lowenheim, 'Electroplating', McGraw-Hill (1978) p. 523.

[12] A. E. Martell and R. M. Smith, 'Critical Stability Constants', Vol. 3, Plenum Press (1977), p. 161.

[13] A. C. West, M. Matlosz and D. Landolt, *J. Appl. Electrochem.* **22** (1992) 301.

[14] Joint Committee on Powder Diffraction Standards, Powder Diffraction File (1972) 6-0696, Iron (α-phase).

[15] For example, H. Sudo, I. Tamura and T. Nishizawa, 'Kinzoku-soshikigaku (Metallography)', Maruzen (1972), p. 161.

[16] J. Horkans, *J. Electrochem. Soc.* **126** (1979) 1861.

[17] H. Freiser and Q. Fernand, 'Ionic Equilibrium in Analytical Chemistry', J. Wiley & Sons, New York (1963).

[18] D. S. Stoichev and S. Rashkov, *C. R. Acad. Bulg. Sci.* **26** (1973) 243.

[19] A. J. Bard and L. R. Faulkner, 'Electrochemical Methods', J. Wiley & Sons, New York (1980), p. 511.